Accepted Manuscript in "Chemical Engineering Research and Design"

HYDRODYNAMICS STUDY OF THE MODIFIED ROTATING DISC CONTACTOR FOR CO_2ABSORPTION FROM NATURAL GAS USING EMULSION LIQUID MEMBRANE

Inamullah Bhatti[a], Abdul Waheed Bhutto[a, b], Khadija Qureshi[a], Khairul Sozana Nor Kamarudin[c], Aqeel Ahmed Bazmi[d,*] and Faizan Ahmad[e]

[a] Department of Chemical Engineering, Mehran University of Engineering and Technology, Jamshoro, Sindh, Pakistan

[b] Department of Chemical Engineering, Dawood University of Engineering and Technology, Karachi, Pakistanabdulwaheed27@hotmail.com

[c] Faculty of Chemical Engineering Universiti Teknologi Malaysia

[d] *Department of Chemical Engineering, COMSATS Institute of Information Technology, Lahore, Pakistan (*ABazmi@ciitlahore.edu.pk)

[e] School of Science and Engineering, Teesside University, Middlesbrough, TS1 3BA United Kingdom (f.ahmad@tees.ac.uk)

*Authors to whom correspondence should be addressed;
Tel: +92-42-111001007 Ext: 152,E-mail: ABazmi@ciitlahore.edu.pk

ABSTRACT

This study modified the rotating disc contactor (RDC) structure to optimize its performance for CO_2 separation from natural gas feed using stable emulsion liquid membrane (ELM). Based on parametric study of absorption of CO_2 from natural gas feed into ELM, the mass transfer behaviour in the RDC system was optimized. Rotor diameter, stator inner diameter and minimum free area of RDC were modified to achieve maximum contact between dispersed liquid phase and gas feed phase which was necessary to achieve maximum mass transfer. The problem of rupture the emulsion droplet due to pressure created by direct dispersing of gas at

the bottom of conventional RDC extraction system was addressed by adding an impeller at the bottom compartment of RDC. Impeller provided continuous mixing of emulsion and a gas sparger was fitted along the impeller side which maintained the dispersed aqueous phase miscible in system. The hydrodynamic behavior of a modified RDC was optimized for CO_2 absorption from natural gas in ELM which indicated that modified design dimensions can provide a maximum liquid- gas contact. Beside the concentration CO_2 in natural gas feed, it was observed that the speed of RDC and run time significantly influences CO_2 absorption from natural gas using ELM. If all the parameters optimized absorption from natural gas feed. This study is also useful in extending the application of RDC in liquid-gas system. In this study are applied in proper conditions, the use of ELM in RDC can be effective for CO_2.

ABBREVIATIONS

DEA	-	Diethylamine
EDS	-	Emulsion Droplet Size
ELM	-	Emulsion Liquid Membrane
GC	-	Gas Chromatograph
h	-	Hour
k	-	Kilo
L	-	Liter
M	-	Molar
MEA	-	Monoethanolamine
m	-	Meter
mL	-	Milliliter
mm	-	Millimeter
mol	-	Mole
NaOH	-	Sodium hydroxide

RDC	-	Rotating Disc Contactor
rpm	-	Rotations per minute
s	-	Second
TEA	-	Triethylamine
w/o	-	Water in oil

NOMENCLATURE

C_{Ao}	-	Final concentration of gas A (kg mol/m)
C_{Ai}	-	Initial concentration of gas A (kg mol/m)
D	-	Mean diameter of emulsion droplet (m)
D_R	-	Rotor diameter (m)
D_s	-	Stator diameter (m)
E	-	Axial dispersion coefficient (m^2/s)
F_r	-	Froude number
f	-	Total holdup of dispersed phase
H	-	Height of column (m)
H_s	-	Compartment height (m)
N	-	Rotor speed (rpm)
N_A	-	Mass flux of pure gas in liquid solution (kg mol/m^2.s)
Q_d	-	Dispersed phase flow rate (mL/min)
Q_c	-	Continuous phase flow rate (mL/min)
Re_F	-	Reynolds number for liquid flow
W_E	-	Weber number
n	-	Agitator speed (rpm)
T	-	Total residence time of the liquid in column (s)
u	-	Phase velocity (m/s)
u_o	-	Characteristic velocity (m/s).

u_c	-	Velocity of continuous phase (m/s)
u_d		Velocity of dispersed phase (m/s)
u_s	-	Slip velocity (m/s)

GREEK LETTERS

ρ_c	-	Density of continuous phase (kg/m)
ρ_d	-	Density of dispersed phase (kg/m)
$\Delta\rho$	-	Density difference (kg/m)
σ	-	Variance
μ	-	Micro

1. INTRODUCTION

RDC was first developed by Shell in the mid 1950's, and since then it is used in numerous applications particularly in system with low interfacial tension(Stevens et al., 2000). The RDCs are simple in construction and provide high throughput with low energy consumption (Mohanty, 2000). Major applications of RDC is in liquid-liquid system (Vikhansky and Kraft, 2004), however its application in gas-liquid system are being explored. They are more efficient and flexible in operation than the conventional sieve-plate, packed and spray columns. Column is more effective for systems with low interfacial tension(Morís et al., 1997). Low performance is major disadvantage of RDC (Morís et al., 1997). Extensive research is being conducted on hydrodynamics and mass transfer behaviour in RDC to improve its performance (Bart, 2003; Chen et al., 2016). Information on hydrodynamic parameters such as the axial dispersion, hold-up and characteristic velocity is important for the scale-up and design of extraction columns

(Morís et al., 1997). Axial dispersion in a RDC depends on the column geometry, rotor speed, continuous and dispersed phase flow rates, and physical properties. The most widely used model for continuous phase axial mixing is the dispersion model developed by Sleicher (Sleicher, 1959) and Miyauchi and Vermeulen (Miyauchi and Vermeulen, 1963). Dispersed-phase hold-up in an RDC depends on the contactor dimensions (column, rotor and stator diameter, and column and compartment height), rotor speed, continuous- and dispersed phase flow rate, and the physical properties of the phases (Strand et al., 1962; Zhang et al., 1985).

In ELM system, NaOH forms layer between the continuous organic phase and the dispersed aqueous phase. Dispersed aqueous phase of ELM acts as carrier to transport the dissolved CO_2 from the gas-liquid interface to the bulk organic phase as shown in **Figure 1**. The reaction of CO_2 with triethanolamine (TEA) occurs in the dispersed phase. In the w/o emulsion, where dispersed aqueous phase contains TEA as reactant and the continuous phase is kerosene, the overall rate of CO_2 absorption is very important. At the gas liquid interface, CO_2 develops contact with NaOH and then it is penetrated inside the droplet and diffused in the extractant. Absorption of CO_2 into aqueous solution of NaOH, along with absorbent such as TEA and DEA has been carried out by several researchers (Park et al., 2004; Park et al., 2008; Takahshi et al., 2005). In these studies it was observed that the rate of CO_2 absorption increases with increase in the concentration of reactants. Both Park et al. (2004) Lin and Chen (2007) reported linear effect of NaOH concentration over CO_2 absorption rate. Similar result was reported by Tedajo et al. (2001).

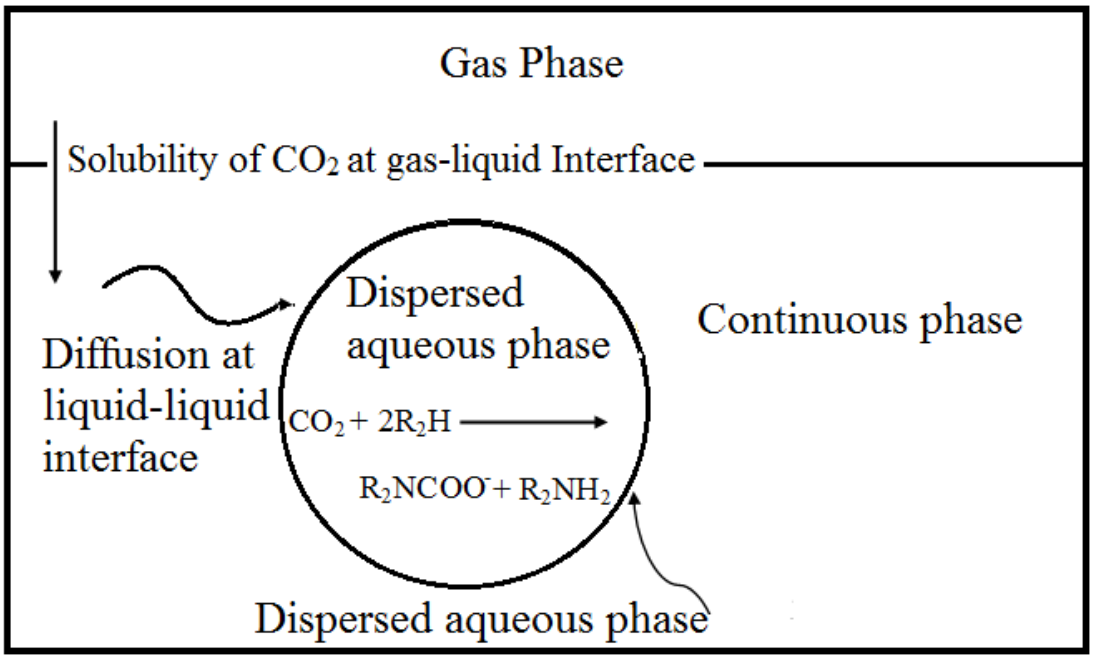

Figure 1. Mass transfer mechanism of w/o emulsion. In ELM system, NaOH forms layer between the continuous organic phase and the dispersed aqueous phase.

This study optimized performance for CO_2 separation from natural gas feed using stable emulsion liquid membrane (ELM) in RDC. In convention RDC it was observed that the flow of gas was very rapid with minimum gas-liquid contact within the system. In order to enhance the mass transfer in dispersed liquid phase and gas feed phase, RDC was modified. The hydrodynamic behaviour of a modified laboratory RDC was studied and optimized. The parameters studied include axial dispersion, hold-up and characteristic velocity for the two-phase system. Considering the initiating role of NaOH over the absorption of CO_2 by ELM in RDC, the effect of molar concentration of NaOH on the absorption of CO_2 was studied and optimum values were obtained.

The effect of RDC speed, time and concentration on the mean molar flux and the effect of TEA concentration on the mass transfer coefficient were analyzed by using the mass transfer principles. Based on mass transfer mechanism the absorption of CO_2 from natural gas feed into the membrane phase of ELM was analysed to determine the mass transfer behaviour of modified RDC and optimize its performance for CO_2 absorption from natural gas feed in ELM.

2. CONVENTION AND MODIFIED RDC COLUMN DESIGN

RDC columns used for gas-liquid system consist of series of stages separated by equally spaced horizontal stators and shaft mounted rotor discs. Liquid injected to the reactor from the top and gas phase is injected through a small gas inlet in the bottom near the rim of the rotor. Discs mounted on the shaft provide larger interfacial contact area to the dispersed phase for maximum mass transfer (Morís et al., 1997). The column consists of vertical segments, in which horizontal stator rings are installed. These stator rings are flat plates with a central opening. In the middle of the compartments formed by the stator rings, the rotor disks are installed. The rotor disks are flat plates attached to a central shaft and driven by an electric motor. Above the top stator ring and below the bottom stator ring the settling compartments are installed. The feed gas and feed liquid inlets are arranged tangentially, in order not to disturb the flow pattern in the inlet compartments. In convention RDC for gas liquid system, it was observed that the flow of gas was very rapid with minimum gas-liquid contact within the system. In order to enhance the mass transfer in dispersed liquid phase and gas feed phase, RDC was modified according to the specifications provided in **Table 1**. Axially, rotating discs mounted on the shaft provides larger surface area to the dispersed phase to increase the interfacial contact area for maximum mass transfer. Since the hydrodynamic behavior of RDC depend on the

entrainment of dispersed phase, holdup and axial mixing the height of RDC, size of compartment and number of compartments to provide maximum contact between gas and liquid were estimated to develop the gas-liquid RDC chamber. In addition, an impeller was added at the bottom compartment of RDC to provide continuous mixing of emulsion.

Table 1. Dimensions of conventional and modified RDC

	Dimensions of conventional RDC	Dimensions of modified RDC
Column Diameter (mm) (6)	120	120
Rotor diameter (mm) (5)	38	40
Rotor thickness (mm) (7)	02	02
Stator inner diameter (mm) (1)	10	15
Minimum free area (%)	50	40
Compartment height (mm) (2)	11	11
Number of Compartments	09	09
Column working height (mm) (8)	148	148

In conventional gas-liquid extraction system, the gas is dispersed under the impeller (Joshi et al., 1982; Poncin et al., 2002). While working with ELM, the direct dispersing gas at the bottom may rupture the emulsion droplet due to its pressure. In the modified RDC system gas sparger was fitted along with the impeller side to maintain the dispersed aqueous phase miscible in the RDC system.

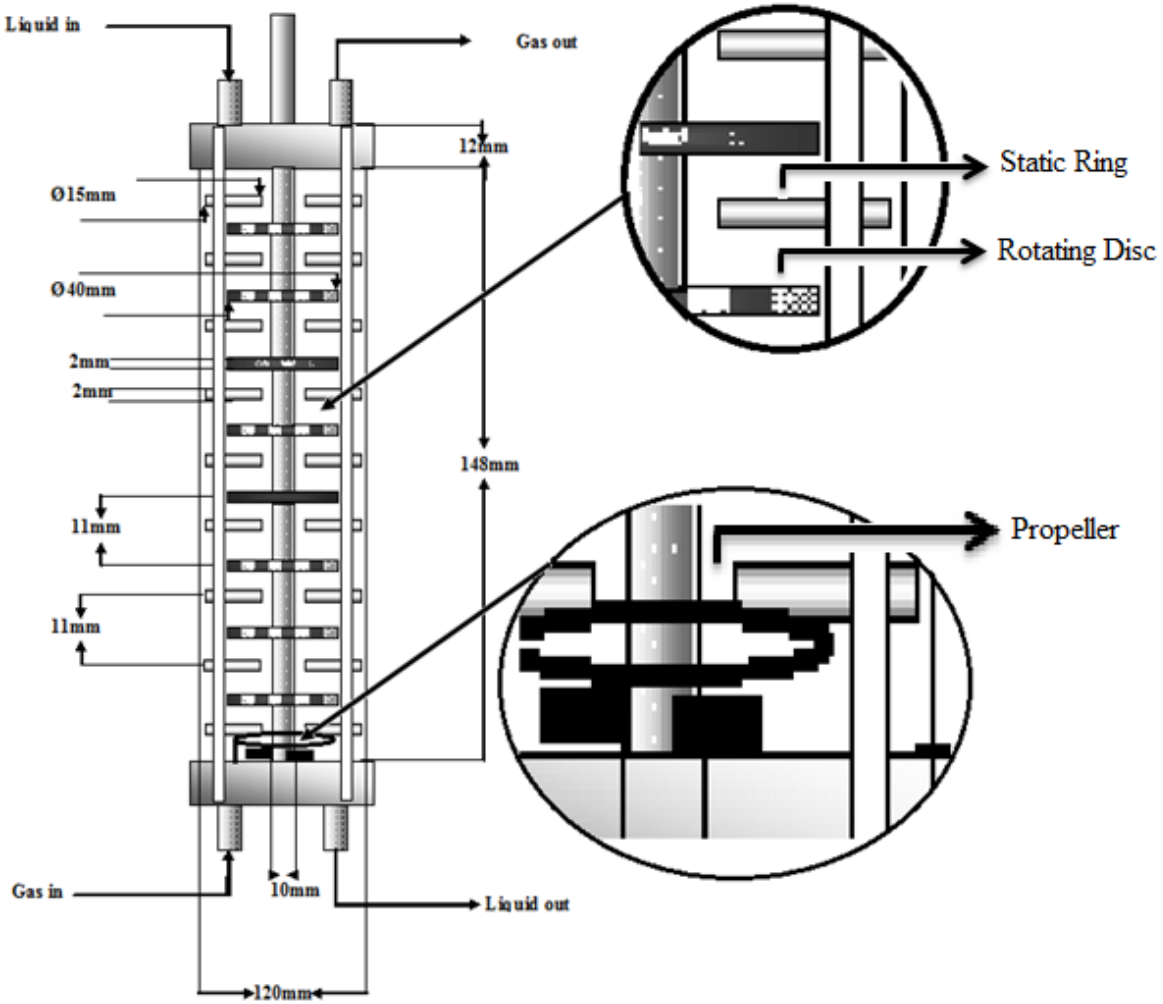

Figure **3.** Modified RDC diagram for gas-liquid system. Upper magnified section shows the close view of modified size of rotating discs and static rings while the lower magnified section shows the close view of propeller added at the bottom compartment of the RDC.

To maintain the hydrodynamic behavior, the RDC was designed with zero horizontal gaps and 11 mm vertical gaps between rotating discs and stationary rings. To provide maximum contact time to gas-liquid, each disc in the compartment of RDC was capable to extend the surface area of dispersed liquid as it shuffled the liquid to replace it for rapid action. Modified RDC system was also designed for counter current flow of gas and liquid. From the bottom side, gas was

dispersed through the spiral tubing shaped gas sparger with small holes to spread the gas. The liquid inlet was placed at the top of RDC to allow the liquid flow on rotating discs. The other dimensions are indicated in **Figure 2** which shows the modified diagram of RDC for the ELM system used in this study. The upper magnified section of the **Figure 2** shows the close view of modified size of rotating discs and static rings of RDC while the lower magnified section shows the close view of propeller added at the bottom compartment of the RDC. **Figure 3** shows the geometry and vortex structures in the RDC(Aksamija et al., 2015).

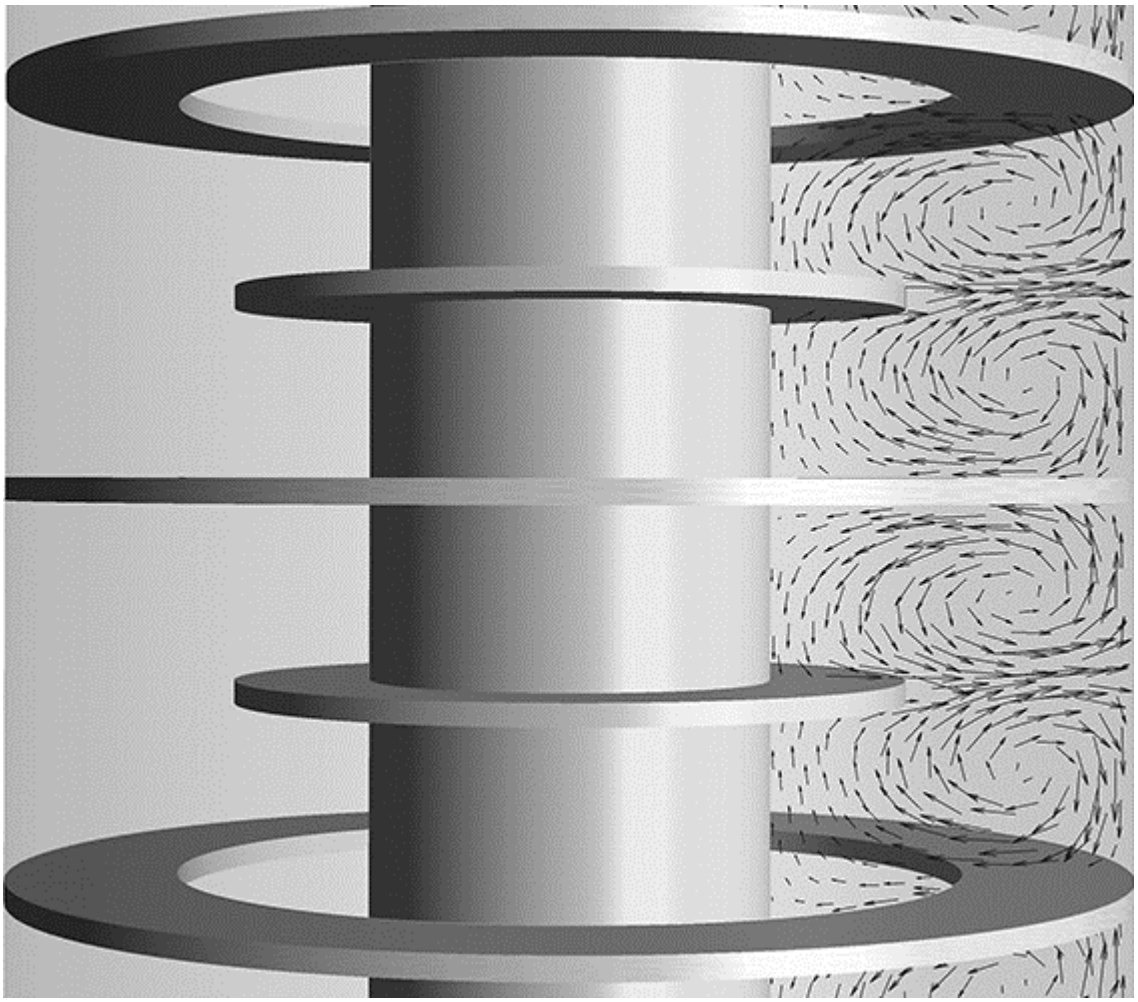

Figure 3. Geometry and vortex structures in the RDC (Aksamija et al., 2015).

3. RESULTS AND DISCUSSIONS

3.1. THEORETICAL CORRELATION OF PARAMETERS

In this section the hydrodynamic parameters include axial mixing, hold-up and characteristic velocity for the two-phase system gas and emulsion liquid were studied in modified RDC and results are discussed with respect to the rotational speed of RDC and the flow rate of the gas and liquid system.

3.1.1. AXIAL MIXING

This model characterizes axial mixing by an axial dispersion coefficient E, which in most cases is accurate enough for design purposes. The axial dispersion coefficient can be determined from the response to a tracer pulse. If the flow is essentially plug flow at the injection and response detection points (closed-closed system), the dispersion modulus can be calculated by Equation (1) (Levenspiel and Smith, 1995) for $[E/(uH)] > 0.01$:

$$\frac{\sigma}{T^2}^2 = 2\left[\frac{E}{uH}\right] - 2\left[\frac{E}{uH}\right]^2\left[1 - e^{\left(\frac{E}{uH}\right)}\right] \quad (1)$$

Where T is total residence time of the liquid in column (s), σ is the variance, E is axial mixing coefficient (m^2/s), u is phase velocity (m/s) and H is the height of column (m).

The flow at the points of tracer injection and response measurement is plug flow, as these points are located before and after the mixing zone. In this study equation (1) was used to calculate the dispersion modulus for one phase flow of emulsion liquid ranging from 5.56×10^{-6} to 1.67×10^{-5} m^3/s and rotor speed between 100 -700 rpm respectively. The experimental results are

shown in **Figure 4**. These results indicates that the dispersion modulus increases linearly with the increase in rotor speed at a constant flow rate, and decreases with increase in flow rates at a constant rotor speed. These results are in agreement with results reported by (Morís et al., 1997; Strand et al., 1962).

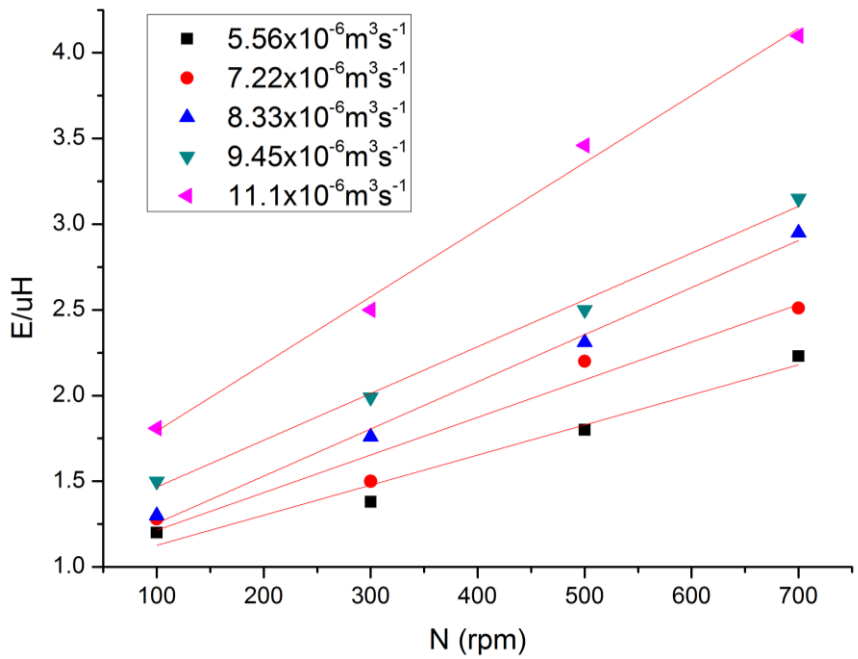

Figure 4. Behavior of dispersion modulus for single phase flow of emulsion liquid (ranging from 5.56 $\times 10^{-6}$ m^3/s to 11.1$\times 10^{-5}$ m^3/s) at rotor speed between 100-700 rpm.

3.1.2. HOLD-UP

Correlation given in equation (2) was used to estimate the overall holdup of RDC (Morís et al., 1997).

$$f = 1.58\left(\frac{nD_R}{u_c}\right)\left(\frac{u_d}{u_c}\right)^{0.96}[(D_S^2 - D_R^2)]^{-0.77}\left(\frac{H}{H_s}\right)^{-0.426}\left(\frac{\Delta\rho}{\rho_c}\right)^{-1.31} Re_f{}^{-0.31} W_E{}^{0.245} F_r{}^{0.96} \qquad (2)$$

Where f is total holdup of dispersed phase, n is agitator speed (rpm), D_R is rotor diameter (m), D_s is stator diameter (m) , u_c is velocity of continuous phase (m/s), u_d is dispersed phase velocity (m/s), H is total height of the column (m) , H_s is compartment height (m) , $\Delta\rho$ is density difference (kg/m), ρ_c is density of continuous phase (kg/m), Re_F is Reynolds number for liquid flow, W_E is Weber number and F_r Froude number.

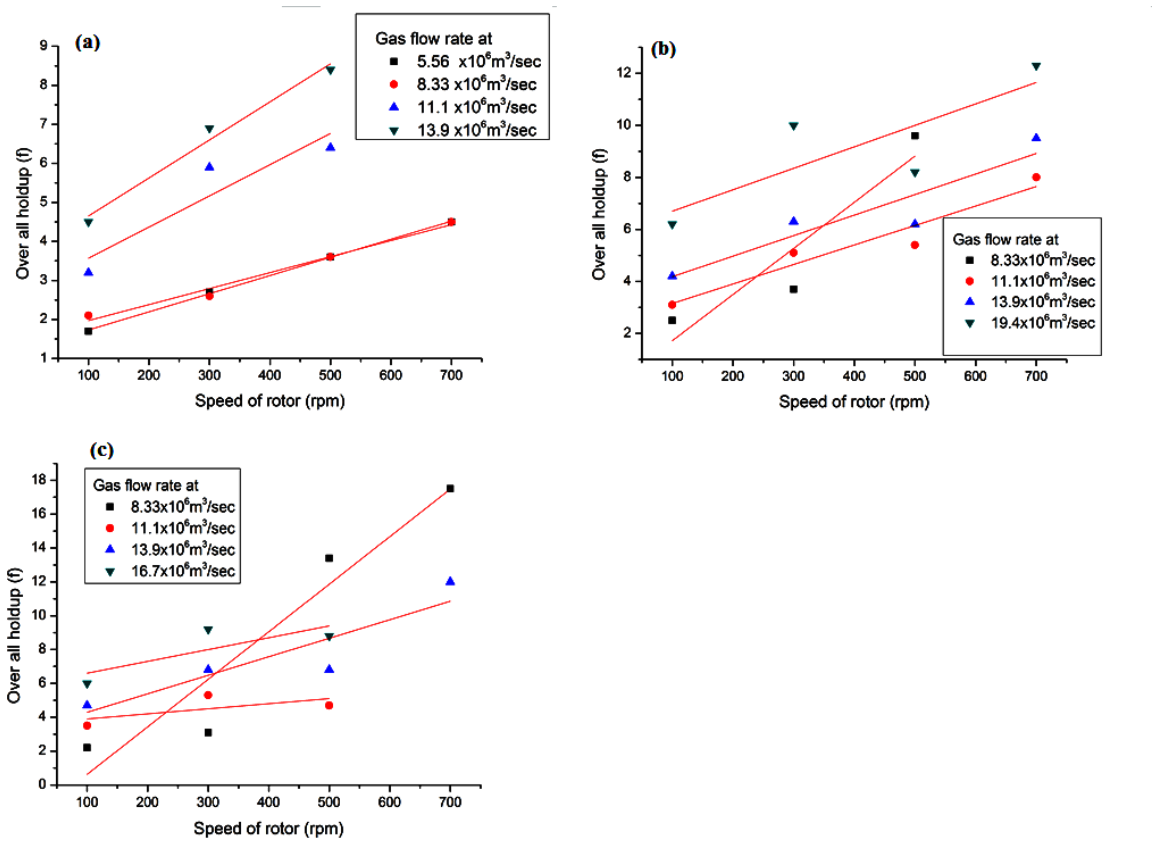

Figure 5. Overall holdup profile of RDC at different gas flow rates for liquid flow rate of (a) $5.56x10^6$ m^3/s, (b) $8.33x10^6$ m^3/s and (c) $11.1x10^6$ m^3/s.

In this study, total dispersed-phase hold-up was measured for aqueous phase flow rates in the range $5.56x10^{-6}$ to $2.22x10^{-6}$ m^3/s, gas-phase flow rates of $5.56x10^{-6}$ to $1.49x\ 10^{-6} m^3/s$ and rotor

speeds of 100, 300, 500 and 700 rpm respectively. Results are given in **Figure 5 (a, b and c)** which shows the linear relationship of rotor speed with the overall holdup for different flow rates of gas in RDC. This was observed that overall holdup increases as rotor speed, total throughput and gas-liquid phase flow ratio increased. These results are in agreement with results reported by (Poncin et al., 2002).

3.1.3. CHARACTERISTIC VELOCITY

Dispersed-phase hold-up is usually correlated with the dispersed and continuous phase superficial velocities by means of a characteristic velocity (u_o) ((m/s). The following equation is used to determine the characteristic velocity (Logsdail et al., 1957).

$$\left(\frac{u_d}{f}\right) + \left[\frac{u_c}{1-f}\right] = u_o(1-f) \tag{3}$$

Relative velocity between the continuous and the dispersed phase flowing counter currently is considered as slip velocity (u_s) (m/s); hence, equation (3) is simplified as under

$$u_s = \left[\frac{u_c}{1-f}\right] + \left(\frac{u_d}{f}\right) \tag{4}$$

The above equation can be further simplified to transform as given below.

$$u_s = u_o(1-f) \tag{5}$$

Equation (5) is most widely used in designing of RDC to determine the rotor speed. For low rotor speeds, the characteristic velocity remains approximately constant as the rotor speed is increased, until a critical speed is reached. Beyond critical speed, the characteristic velocity decreases as the rotor speed increases. This region corresponds basically to counter current

flow without drop breakage. While after critical speed corresponds to drop breakage caused at high rotor speeds. For plotting the data, equation (5) can be expressed as:

$$f u_s = f(1-f)u_o \tag{6}$$

In this study the results obtained by using the equations (6) are plotted in **Figure 6** to show the effect of rotor speed on the velocity characteristics. The relation shows that at 700 rpm the velocity characteristic is more fit to the linear trend of increment. By plotting data of (fu_s) versus [f(1-f) u_o] for a given rotor speed and fitting the data to a straight line by least squares, the slope corresponds to the characteristic velocity (u_o.) This increase in data scattering, especially for low rotor speeds, can be observed in **Figure 6**. It indicates that at rotor speed of 700 rpm maximum gas–liquid interfacial contact occurred.

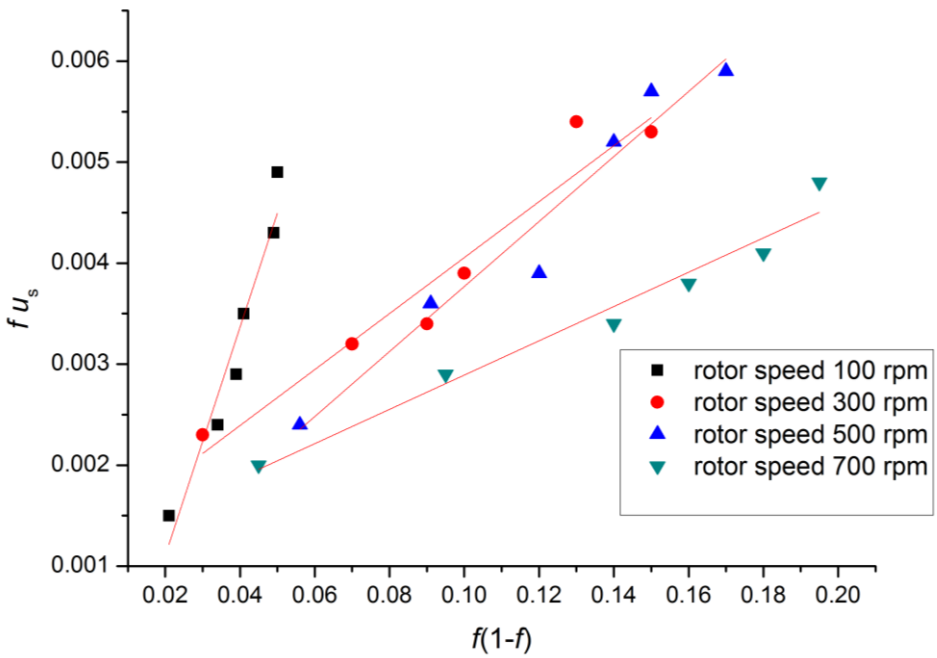

Figure 6. Effect of rotor speed on characteristic velocity of RDC

3.2. EXPERIMENTAL CORRELATION OF RESULTS

3.2.1. EFFECT OF ROTOR SPEED ON DROP SIZE DISTRIBUTION

The drop diameters determined in the analysis of the two-phase mixture were used to establish the corresponding drop size distributions considering 10 equally spaced size classes in the range $1.0 \leq d\ (\mu m) \leq 10.0$ for all analyzed operating conditions. For a dispersed phase flow rate (Q_d) of 70 mL/min, the volume of emulsion liquid fed to the column was not large enough to promote a well-distributed flow of drops in space. Flooding was not observed since the continuous phase flow rate is always equal to zero, so that the emulsion liquid ended up accumulating below the stators, which resulted in the appearance of very large drops along the column. Even though the increase in the rotor speed reduced the thickness of the emulsion layer, this effect was not significant enough to prevent drops from coalescing in the vicinity of the stators.

At low rotor speed, organic phase is accumulated not only below the stators but also below the discs. However for dispersed phase, at different flow rates considered, the layer of emulsion liquid below column stators was very small, and more uniform drop flow patterns along the column were observed. Therefore, due to the differences in the operation regime, the results for dispersed phase flowrate (Q_d = 50mL/min) were not taken into account for assessing the effects of operating variables on drop size distributions. Considering two distinct positions along the RDC column (stages 5 and 9), the drop size distributions determined for three different rotor speeds are reproduced in **Figure 7 and 8 (a, b and c).**

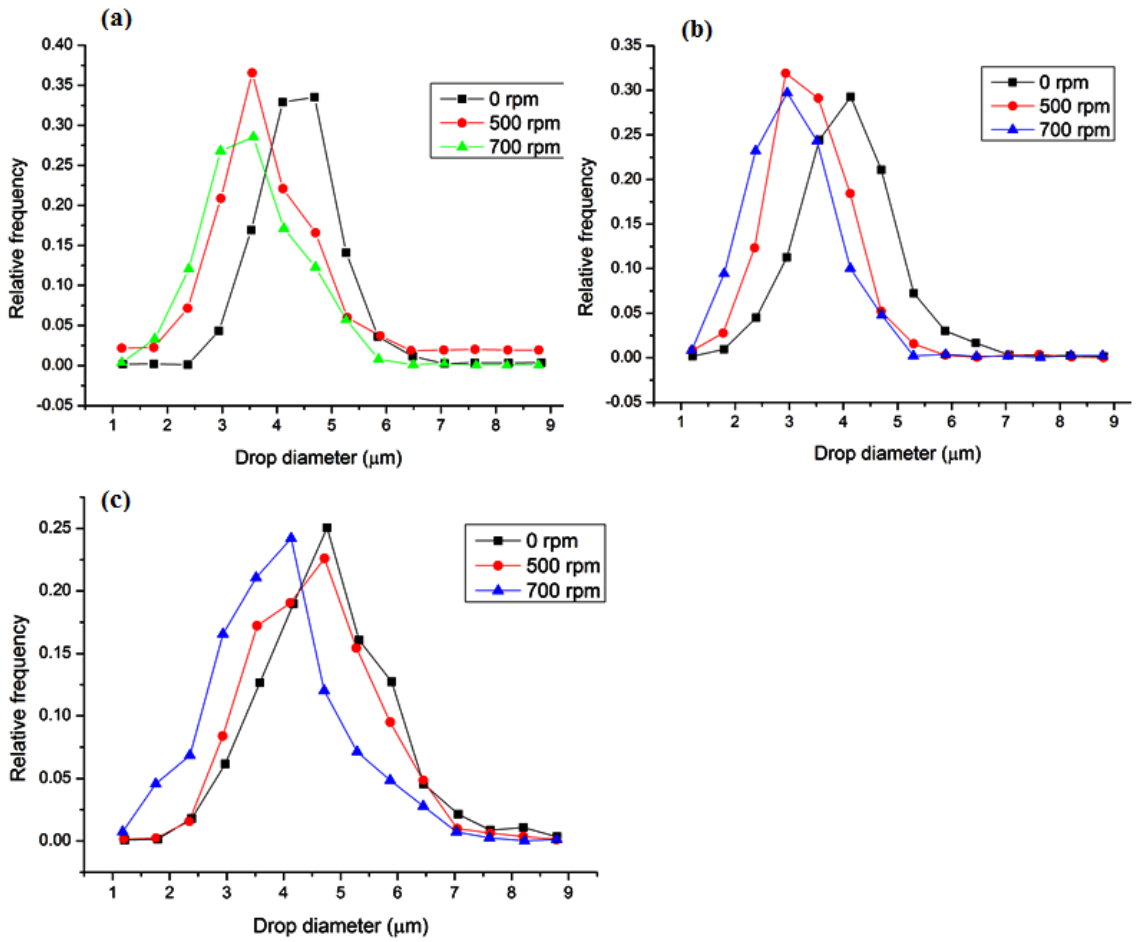

Figure 7. Effect of rotor speed on drop size distribution at stage 9 for dispersed phase flow rate (Q_d) of (a) 50 mL/min, (b) 250 mL/min and (c) 500 mL/min.

In the case of all values of Q_d, the size distribution in either stage clearly shifts towards the left upon an increase in the rotor speed, evidencing drop breakup. The shear energy imposed by the rotating discs on the drops during their ascension accounts for this breakup, and, since such energy grows with the rotation speed, so does the drop breakup frequency, shifting size distributions towards smaller diameters and therefore leading to higher superficial area values. Even in stage 0, which comprises the region between the distributor and the first stator (stage

1), where there is actually no rotating disc, the size distributions seem to be affected by the rotor speed, as evidenced by the results presented in **Figure 8**. In this stage, since there were no internal parts on which the organic phase could accumulate, the results related to Q_d = 70 mL/min have also been considered. Contrary to the observation of the rest of the RDC column, when the rotor speed augments, the drop size distribution in stage 0 shifts to the right, towards larger diameters. This effect is clearly perceived for the lowest Q_d value and seems to become less pronounced as the organic flow rate grows.

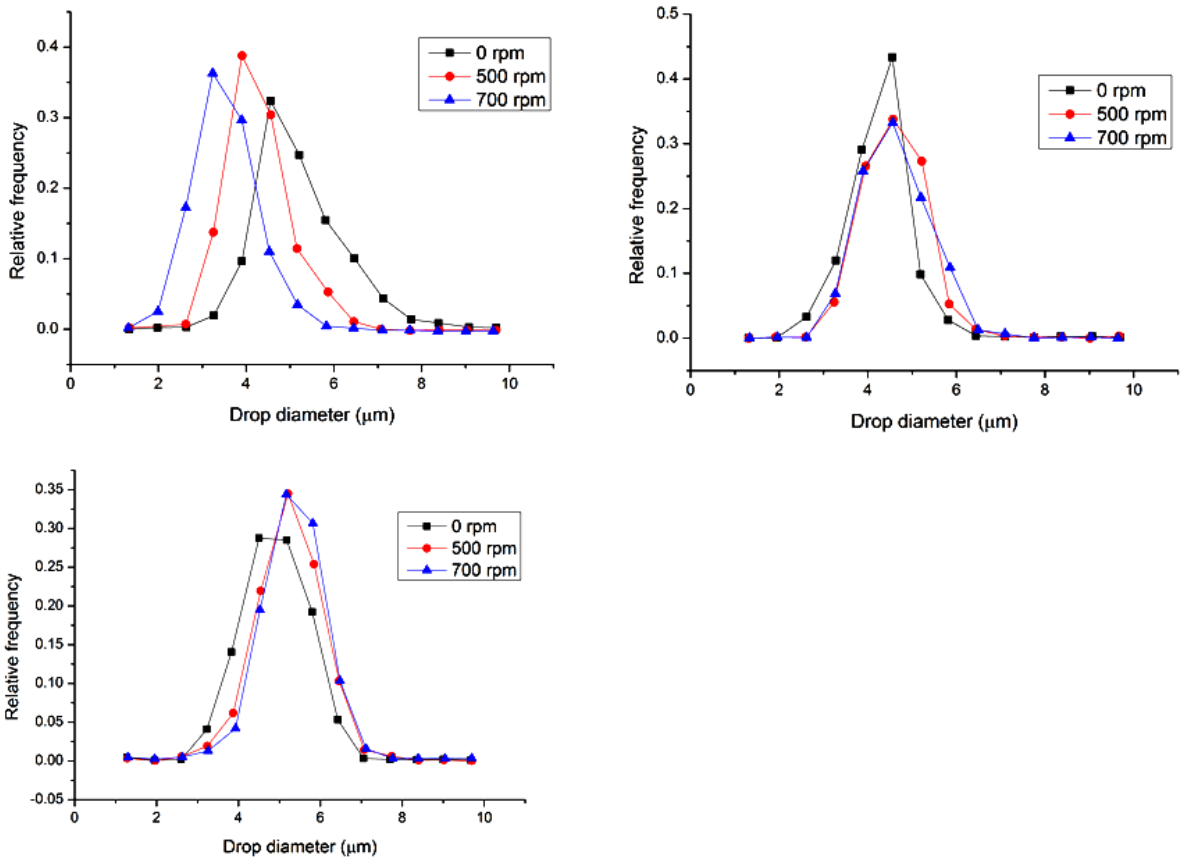

Figure 8. Effect of rotor speed on drop size distribution at stage 0 when dispersed phase flow rate is (a) Q_d=50 mL/min, (b), Q_d=250 mL/min and (c) Q_d=500 mL/min.

As the drop formation diameter at the distributor is fixed for a given Q_d, these changes in the size distribution can stem only from coalescence. Visual observations during column operation indicate that, as a result of the disc rotation, a central vortex is formed in stage 0, dragging drops towards it and thereby favoring their coalescence. The smaller the drop ascension velocity the easier it will be for the vortex to capture this drop. Such behavior is consonant with the fact that the intensity of the rotor speed effect seemed to decrease with the dispersed emulsion liquid phase flow rate, since the drop formation diameter and, accordingly, its ascension velocity grows with Q_d.

3.2.2. EFFECT OF COLUMN HEIGHT ON DROP SIZE DISTRIBUTION

Column height was the one of the variable evaluated for its effect on drop size distribution. **Figure 9 (a, b and c)** shows size distributions at three different points along the RDC column measured for two values of emulsion phase flow rate and rotor speed. These results provide the clear evidence of strong variation in the drop size along the column height, indicating the intrinsic difficulty in defining a reliable mean drop size for the whole equipment. Due to the drop breakup promoted by the rotating discs, the size distributions are progressively shifted towards smaller diameters. This effect is particularly pronounced in the case of the higher Q_d value, at which the size distributions at the top and the bottom of the column differ considerably from each other.

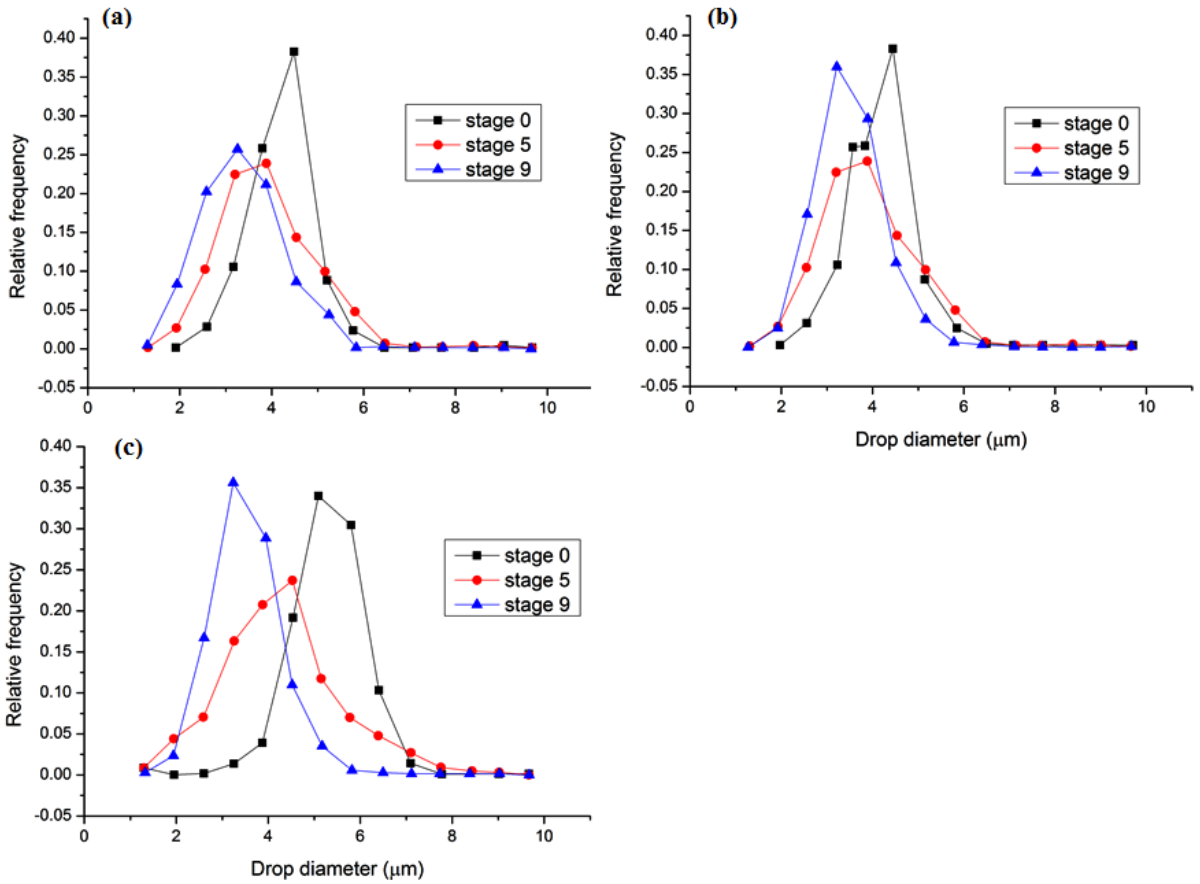

Figure 9. Effect of column height on drop size distribution at stage 0, 5 and 9 when N = 500 rpm and Dispersed phase flow rate is (a) Q_d = 50 mL/min, (b) , Q_d = 250 mL/min, (c) Q_d = 500 mL/min.

3.2.3. CHANNELLING AND FLOODING IN RDC

In RDC the available contact area remains undisturbed even at a high or low flow rate because the two fluid flows are independent. The amount of the emulsion liquid and the gas was varied in the range of 5.56×10^{-6} to $19.4 \times 10^{-6} m^3.s^{-1}$ and 5.56×10^{-6} to 13.9×10^{-6} $m^3.s^{-1}$ respectively. Because of the independent flow path in each rotating compartment channeling was not observed.

The flooding rate represents the maximum volumetric capacity of a contactor under a given set of conditions. In this study, flooding was characterized by flow rates of emulsion liquid and gas at 300, 500 and 700 rpm of rotor speed. Both the dispersed phase and the continuous phase flow rates were recorded at the flooding point. As a check, the dispersed phase flow rate was decreased by about 10% to allow the column to revert to normal operation, and then increased until flooding reoccurred. Intense phase mixing was observed immediately prior to the onset of flooding. In RDC flooding was more easily recognizable at high agitator speeds as shown in **Figure 10**. Under these conditions, the droplets entering the first compartment were quickly ruptured to produce very small drops of the order of 0.5 μm to 1 μm.

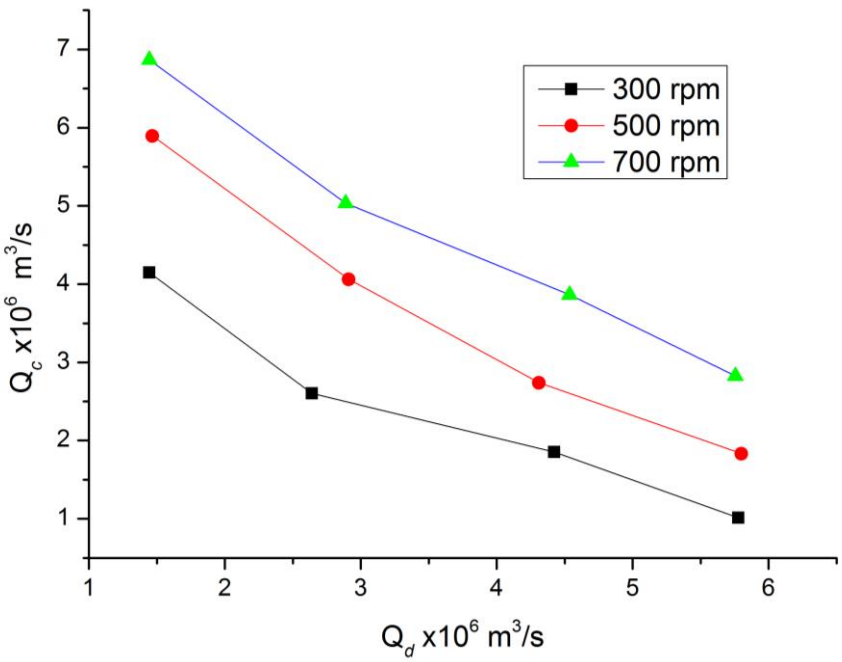

Figure 10. Flooding data of RDC for emulsion liquid-gas system for different flowrates of continuous and dispersed phase.

The terminal velocities of these droplets were very much less than the downward velocity of the continuous phase, and the droplets were therefore carried out of the column with the continuous phase. Flooding was easily recognizable with the emulsion liquid-gas system.

3.2.4. PRESSURE DROP IN RDC

Figure 11 shows the pressure differences in the bottom, top and central stages of the RDC with a liquid phase and gas phase together. The pressure at the rim of the RDC is always higher than near the axis, due to the centrifugal pressure. The pressure thus increases from the axis on top of the disc to the rim of the reactor (ΔP_{top}), up to 5 psi at 700 rpm. The pressure decrease between the rim of the reactor and the axis below the rotor (ΔP_{bottom}) is large, up to 25 psi at 700 rpm. The difference is the pressure drop per stage (ΔP_{center}), which is thus up to 12 psi at 700 rpm. The pressure drop is not caused by the friction of the fluid, as would be the case in the flow between two flat plates. The centrifugal pressure plays a large role, as is seen by the influence of the rotational disc speed. The liquid flow rate has a large influence as well. The pressure drop per stage in the case of a liquid flow rate (6.7×10^{-6} m^3/s), is 7 psi at 700 rpm of RDC, which is an order of magnitude lower. ΔP_{top} = 25 psi, at 700 rpm, in this case, and ΔP_{bottom} is thus almost the same. If no liquid flow rate would be present, no pressure drop over a stage would be expected of course, since the buildup of centrifugal pressure is then the same above the rotor as below the rotor. In the case of a (large) liquid flow rate, the pressure buildup above the rotor will be lower, due to the centrifugal flow, while the pressure will decrease more below the rotor, where the flow is centripetal.

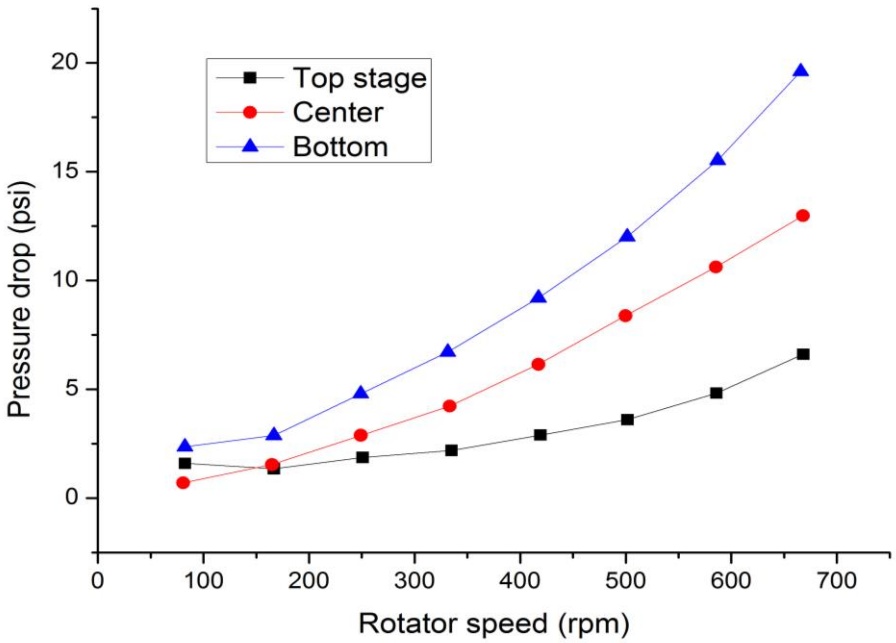

Figure **11.** Pressure drop at top, bottom and center of RDC as function of rotator speed *(N)*.

3.3. EFFECT OF TEA CONCENTRATION ON ABSORPTION OF CO_2

In this study the basic principles of emulsification were followed in the emulsion preparation. Both organic phase and the aqueous phase were prepared separately and then the aqueous phase was dispersed in the organic phase to form w/o ELM. Aqueous phase was prepared by dissolving extractant into NaOH solution. Pre-emulsion aqueous phase was prepared using 0.1, 0.2, 0.3, 0.4 and 0.5 M of NaOH. Organic phase was composed of organic diluents and the surfactant. Kerosene was used as organic phase and TEA/diethylamine (DEA) were dissolved in internal aqueous phase as extractant. To increase the stability of ELM, Span-80 (sorbitan monooleate with a molecular weight of 428) was used as surfactant. To analyze the effect of amine concentration on absorption of CO_2, the samples of ELM using 2, 4 and 6% v/v of TEA were prepared separately. The selected samples were applied in the modified RDC system to

determine the performance of amine based w/o emulsion for absorption of CO_2 absorption. RDC was operated at 300 rpm and for 30 minutes. Absorption results for each sample were analyzed by gas chromatography. The results are recorded in **Table 2** for both DAE and TEA which shows that concentration of the reactant influences the absorption of CO_2. Increasing the amine concentration in dispersed phase of ELM, the amount of CO_2 absorbed increased with respect to its volume. This result in **Table 2** shows that TEA is more effective than DEA. DEA is a secondary amine and two mole of primary and secondary amines react with one mole of CO_2 to form carbamate and bicarbonate according following equation (Wan et al., 2001).

$$CO_2 + 2R_2NH \longrightarrow R_2NCOO^- + R_2NH_2 \quad (7)$$

However, tertiary amine (like TEA) does not form carbamate, but it function as homogeneous base catalyst for CO_2 hydrolysis. As previously mentioned by Park et al. (2006), the catalytic behavior of the TEA in ELM increases the reaction rate constant, thus increases the amount of CO_2 absorbed in RDC. Another important factor is the emulsion droplet size (EDS). Smaller droplets of ELM provide large surface area to absorb more amount of CO_2 in the RDC system. It was observed that EDS of ELM containing TEA was smaller than the DEA, which also increased the amount of CO_2 absorbed by the emulsion containing TEA compared with ELM containing DEA.

Table 2. Absorption of CO_2 from pure CO_2 using DEA and TEA

NaOH	DEA	CO_2 Absorption		TEA	CO_2 Absorption	
M	% v/v	% mole	Mole	% v/v	% mole	mole
	2	83.17	0.8317	2	89.00	0.8900
0.1	4	88.65	0.8865	4	94.25	0.9425
	6	89.53	0.8953	6	96.54	0.9654
	2	96.9	0.9690	2	97.03	0.9703
0.2	4	97.77	0.9777	4	97.20	0.9720
	6	98.16	0.9816	6	97.54	0.9754
	2	98.62	0.9862	2	97.64	0.9764
0.3	4	98.84	0.9884	4	97.65	0.9765
	6	99.32	0.9932	6	97.97	0.9797
	2	99.36	0.9936	2	98.49	0.9849
0.4	4	99.42	0.9942	4	98.53	0.9853
	6	99.45	0.9945	6	99.42	0.9942
	2	99.64	0.9964	2	99.49	0.9949
0.5	4	99.98	0.9998	4	99.68	0.9968
	6	99.99	0.9999	6	99.99	0.9999

3.4. EFFECT OF NAOH ON CO_2 ABSORPTION

The samples of ELM using 2% TEA and DEA were prepared separately with various NaOH molarities to determine the effect of NaOH concentration on the CO_2 absorption in the modified RDC system operated at 300 rpm and for 30 minutes. The moles of CO_2 absorbed by w/o emulsion for both TEA and DEA are given in **Table 2** which indicates that increasing NaOH concentration in dispersed aqueous phase increases CO_2 absorption for both TEA and DEA. By increasing the molar concentration of NaOH, the mass transfer coefficient was increased, which enhanced CO_2 absorption by dispersed aqueous phase of ELM in RDC system.

4. OPTIMIZATION OF PERFORMANCE OF MODIFIED RDC FOR CO_2 ABSORPTION FROM NATURAL GAS USING ELM.

Above discussion suggested compared to DEA, TEA is more efficient as an extractant for CO_2 absorption in RDC using ELM. In following section separation of CO_2 from CO_2/CH_4 gas feed using ELM containing TEA as an extractant in modified RDC system was analyzed. Various samples of emulsion were prepared using the specifications given in **Table 3** while emulsification speed and time was fixed for all samples at 20,000 rpm and 120 minutes respectively. These samples were used to investigate the CO_2 absorption behavior from the gas feed in ELM using modified RDC. In modified RDC, the ratio of CO_2 and CH_4 in gas feed was controlled by controlling the flow rate and pressure of these gases entering the RDC. After introducing ELM in RDC, CO_2 was entered at 8 L/h at 25 psi and 25°C and CH_4 was entered at 6.5 L/h at 25 psi and 25°C to obtain a CO_2/CH_4 ratio of 0.55/0.45 for respectively. Using these parameters the moles of CO_2 and CH_4 were calculated using the ideal gas law. According

to stoichiometric calculations under above conditions CO_2 and CH_4 in the RDC were 55 and 45 mole % respectively.

Based on the one mole of gas the study was carried out to analyze the effect of time, concentration and speed of RDC on CO_2 absorption in ELM. The behavior of CH_4 was assumed inert in the ELM system while physical absorption of CO_2 from the gas mixture was evaluated experimentally by using gas chromatography. Agilent Gas Chromatograph (GC) A30000 was used to analyze the CO_2 absorption in RDC system. Cerity QA-QC software was used to get the computer generated report for amount of CO_2 and CH_4 present in the exit gas stream from RDC system.

Table **3**. Specification of w/o Emulsion

Phase Composition	Specifications
Membrane phase	30°C at 700 rpm for 15 minutes
Kerosene	100 ml
Span-80	4% v/total volume
Internal stripping phase	30°C at 700 rpm for 15 minutes
Water	100 ml
NaOH	0.2M
TEA	2, 4 and 6% v/water volume

4.1. CO_2 ABSORPTION CAPACITY OF ELM

Mass transfer flux and the coefficient of mass transfer are the important properties in determining the behavior of absorption system. Agitation speed, operational time and the concentration of the absorbent are key factors which determine the mass transfer mechanism. In RDC system, CO_2 absorption capacity of ELM depends on concentration of extractant in dispersed aqueous phase and the contact time between feed gas and emulsion liquid. In this study the effect of TEA concentration, time and RDC speed on the absorption of CO_2 of ELM was analyzed to determine the optimum values.

4.1.1. EFFECT OF RUN TIME ON CO_2 ABSORPTION

Studies by Hagewiesche et al. (1995) and Brogren and Karlsson (1997) on CO_2 absorption in aqueous solution using scrubbers or gas-liquid absorber, also showed CO_2 absorption increases with mean residence time. Experiments were conducted in modified RDC to optimize agitation time for maximum CO_2 absorption in ELM in batch process. The sample of outgoing gas stream from the RDC system was introduced to GC at 5 minutes interval. The amount of CO_2 absorbed by the ELM in RDC was calculated based on CO_2 present in the outgoing stream subtracted from the total CO_2 feed to the RDC. The speed of RDC was fixed at 300 rpm for each sample. The effect of time on absorption of CO_2 in ELM from gas mixture of CO_2 and CH_4 was assessed for 2, 4, and 6% v/v of TEA. Results are given in **Table** 4. These results shows that for all concentrations of TEA, increasing the retention time in RDC, increases the CO_2 absorption in ELM. Maximum CO_2 absorption of 4.602 kmol/m^3 was achieved with 2%

(v/v) TEA when contact time between feed gas and the aqueous dispersed phase of ELM was extended to 60 min.

Table **4.** The amount of CO_2 absorbed by the ELM in modified RDC

TEA % v/v	Time (min)	CO_2 absorption (kmol/m^3)						
		30	35	40	45	50	55	60
2		4.548	4.551	4.563	4.572	4.579	4.591	4.602
4		5.140	5.143	5.201	5.206	5.223	5.265	5.276
6		5.477	5.477	5.478	5.479	5.479	5.481	5.482

4.1.2. EFFECT OF TEA CONCENTRATION ON CO_2 ABSORPTION

The CO_2 absorption per volume of ELM were plotted against the concentration of TEA in the dispersed aqueous phase of ELM in the **Figure 12** for of RDC speed of 300, 500 and 700 rpm calculated after 30 minutes operation. It was observed that CO_2 absorption increased with increasing the concentration of TEA in the dispersed aqueous phase of ELM. **Figure 12** shows that at speed of 300 rpm in RDC, 4.6 kmol/m^3 of CO_2 was absorbed by the ELM using 2% v/v of TEA, whereas using 6% TEA concentration in ELM, the absorption of CO_2 increased to 5.5 kmol/m^3. The similar effect of TEA concentration on the absorption of CO_2 in ELM was observed in RDC system operated at 500 rpm and 700 rpm as shown in **Figure 15 (b and c**).

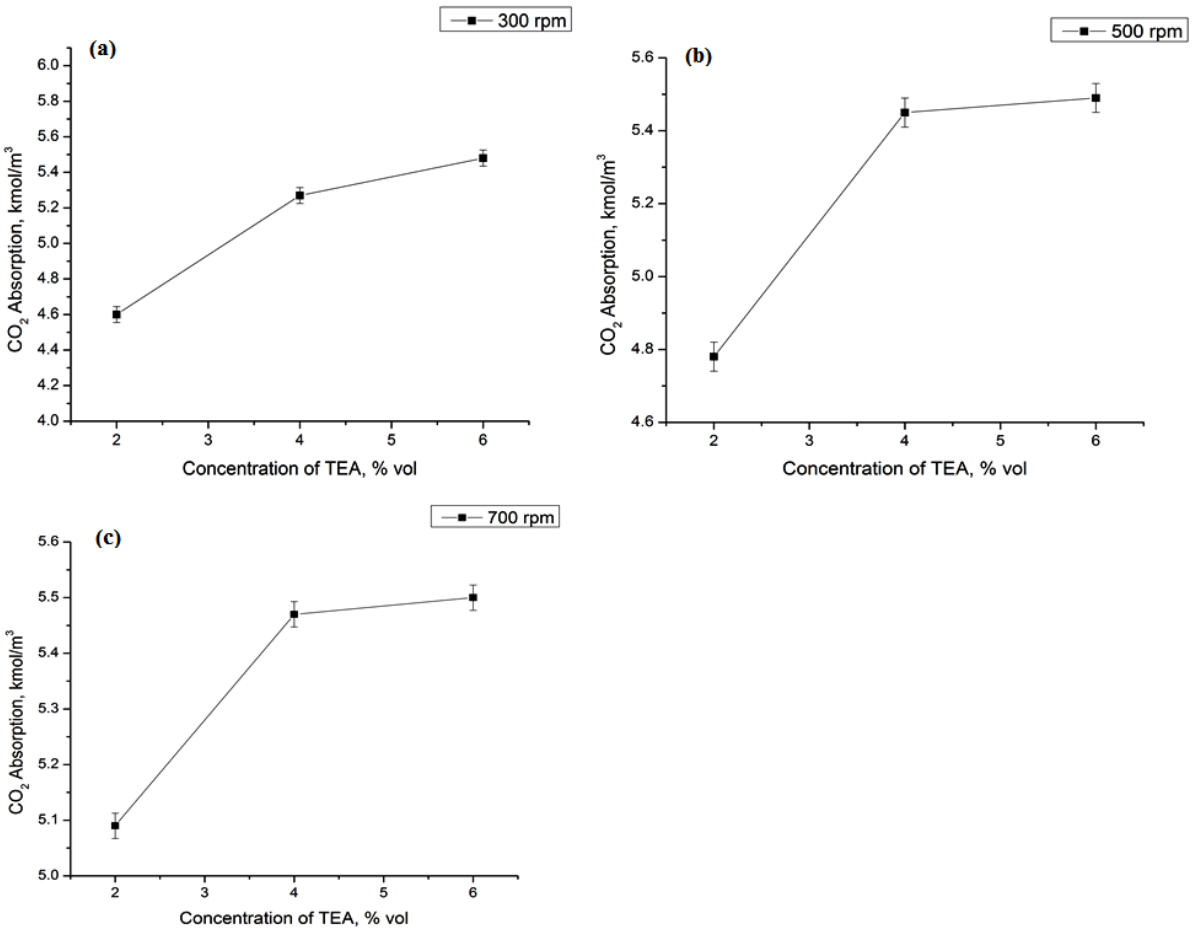

Figure 12. Effect of TEA on absorption, RDC speed of (a) 300 rpm for 30 min, (b) 500 rpm for 30 min and (c) 700 rpm for 30 min.

Significant increase in CO_2 absorption was observed when TEA concentration was increased from 2% to 4%, but the absorption of CO_2 was increase slightly as the concentration of TEA was increased from 4% to 6%. These results suggest that up to TEA concentration of 4% in ELM, the RDC system is effective to absorb maximum amount of CO_2 from gas mixture of CO_2/CH_4. The higher concentration of absorbent in the dispersed aqueous phase of ELM promote absorption of CH_4 which reduces the CO_2 absorption efficiency of ELM. Earlier

Rubia et al. (2010) reported that the concentration of TEA has linear influence on the CO_2 absorption in gas-liquid interface of bubble size. study by Donaldson and Nguyen (1980) on the chemical reaction kinetics of the CO_2 with TEA in gas-liquid contact system also found that reaction rate increased with increase in the concentration of TEA.

4.1.3. EFFECT OF RDC SPEED ON CO_2 ABSORPTION

The effect of RDC speed on absorption of CO_2 using ELM in RDC system is reported for the first time and the effect of speed of modified RDC on CO_2 absorption is compared with the rotating packed bed and stirred autoclave reactor in gas-liquid system. The effect of RDC speed over the absorption of CO_2 was observed at 300, 500 and 700 rpm for 30 minutes. The results effect of RDC speed on the absorption of CO_2 for 2, 4 and 6% v/v of TEA are plotted in the **Figure 13** which **s**hows CO_2 absorption linearly increased with increase in the speed of RDC from 300 to 700 rpm. For ELM containing TEA 2% v/v, the amount of CO_2 absorbed was 4.60 kmol/m^3at 300 rpm, whoever when RDC speed was increased to 700 rpm, the amount of CO_2 absorption increased to 5.09 kmol/m^3. CO_2 absorption increased from 5.3 to 5.5 kmol/m^3 for ELM containing 4% v/v of TEA when RDC speed was increased from 300 rpm to 700 rpm **(Figure 13(b))**. . In case of 6% v/v of TEA in ELM, the linear increase in the CO_2 from 5.48 kmol/m^3 to 5.55 kmol/m^3 when RDC RDC speed was increased from 300 rpm to 700 rpm as shown in **Figure 13 (c)**. These results showed that the speed of RDC also influences absorption of CO_2. Earlier studies also suggest that increasing the speed of rotating packed bed and stirred autoclave reactor the efficiency of CO_2 separation was improved (Albal et al., 1983; Chaudhari et al., 1987; Karandikar et al., 1986; Ledakowicz et al., 1984; Lekhal et al., 1997 ; Lin and Chen, 2007; Lin et al., 2008). High speed of RDC developed rapid contact

between dispersed aqueous droplets and the feed gas. As speed increases, the contact between the gas and the liquid increases, thus it provides rapid diffusion of gas at the liquid interface.

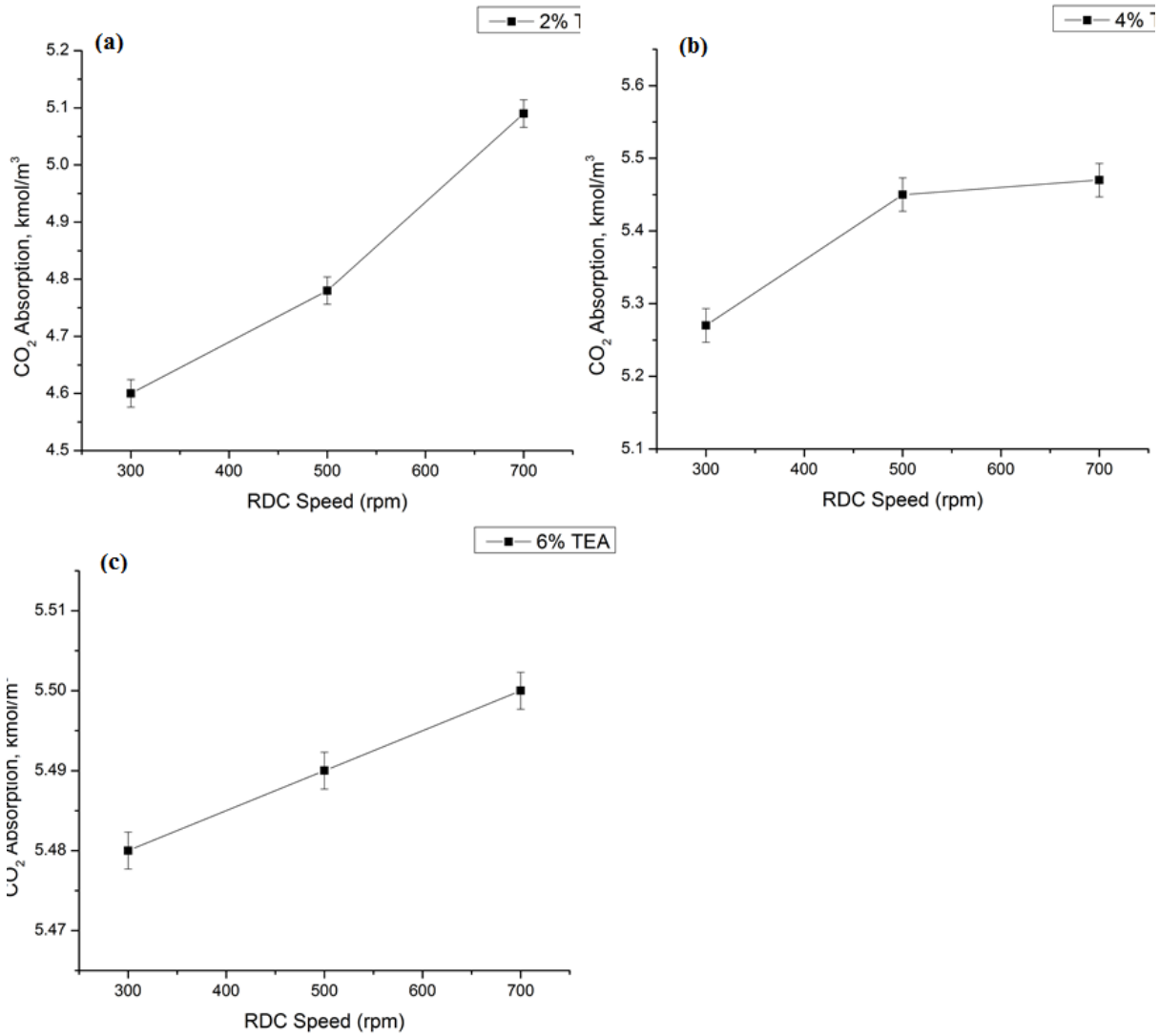

Figure 13. Effect of RDC speed on absorption using (a) TEA 2% v/v., (b) TEA 4% v/v and (c) TEA 4% v/v

The operating behavior of RDC speed showed that maximum contact area was provided to gas feed with dispersed aqueous phase. The discs rotated the emulsion droplets inside the RDC

and while increasing the speed of RDC the rate of CO_2 absorption was increased due to the maximum contact between gas and the dispersed aqueous droplets containing TEA.

4.2. MASS TRANSFER COEFFICIENT OF CO_2 IN MEMBRANE PHASE OF ELM

In following section effect of RDC speed, time and concentration on the mean molar flux and the effect of TEA concentration on the mass transfer coefficient were analysed in modified RDC using the mass transfer principles. Available design of modified RDC provided the analysis of mass transfer at top stage; hence it was not possible to analyze the concentration difference at each stage to calculate the individual mass transfer coefficient.

4.2.1. THE EFFECT OF TEA CONCENTRATION ON THE MEAN MOLAR FLUX

To determine the effect of TEA concentration on the mean molar flux, the absorption rate of CO_2 from gas mixture of CO_2/CH_4 in ELM was calculated by applying following equation for 0.5, 1.0 and 1.5 kmol/m^{3}concentration of TEA in ELM. The equation is based upon the penetration theory first presented by Higbie (Higbie, 1935a, b; Park et al., 2006).

$$N_A = \left(C_{A_i} - C_{A_o}\right)\sqrt{D/\pi t} \qquad (8)$$

Where N_A (kg mol/m^2.s) is the rate of mass transfer rate of pure gas in liquid solution per unit area of surface, C_{Ai} (kg mol/m^3) is the initial concentration of gas A entered in to the RDC and C_{Ao} (kg mol/m^3) is the final concentration of gas A analyzed by GC, D is mean diameter of emulsion droplet (m) and t is the contact time (s).

The experimental conditions were fixed at RDC speed of 700 rpm speed and 30 minutes operational time for each sample. **Figure 14** shows the results of the mean molar flux of CO_2 against the concentration of TEA in ELM. The results indicated that the mean molar flux for CO_2 increased with increase in the concentration of TEA. This is due to the fact that the reaction rate constant of CO_2 for the TEA increases with increase in concentration of reactant. Earlier Donaldson and Nguyen (1980) conducted experiments on the reaction kinetics and transport behavior of CO_2 in aqueous amine solutions and concluded that the TEA concentration has linear relation with CO_2 molar flux and the reaction rate. In the dispersed aqueous phase of ELM, un-protonated TEA functions as base catalysis for hydration of CO_2 to form bicarbonate therefore due to the pseudo-first order rate constant and the relation of TEA concentration will be linear to the CO_2 molar flux.

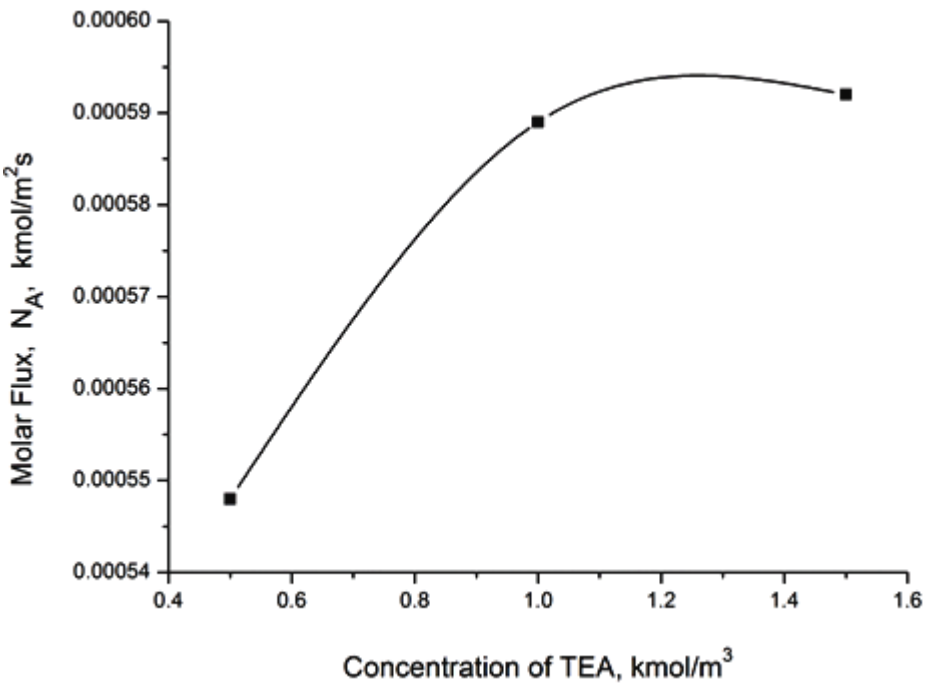

Figure 14. Effect of TEA concentration on mean molar flux

Keeping the mean diameter of droplet remains constant, the concentration of TEA was increased for each droplet of ELM. Increasing the concentration of TEA in dispersed aqueous phase of the ELM increased mean molar flux of TEA. The increase in concentration gradient provides more compartments in each of the emulsion droplet to diffuse significant amount of CO_2. High concentration of TEA makes the ELM more effective to diffuse CO_2 in the ELM. Increasing concentration of TEA decreases the stability of emulsion due to increase in the interfacial surface tension of the emulsion droplet. Therefore, it is necessary to select the concentration of TEA according to the stability characteristic of ELM**.** The stability analysis suggested that emulsion below 11.5 pH value was 100% stable. According to **Figure 14**, 1.4 kmol/m^3 of TEA is highly suitable in ELM according to its stability, since the rate of mass transfer of CO_2 was $5.95x10^{-4}$ kmol/m^2.s. Further increasing concentration of TEA in the ELM slight reduces the rate of mass transfer of CO_2 because of the instability of ELM.

4.2.2. EFFECT OF RDC SPEED ON MEAN MOLAR FLUX

In many gas-liquid transport systems stirring rate influences the rate of diffusion (Vladimir, 2010). Experimental studies were carried to analyse the optimum RDC speed for maximum CO_2 absorption in the dispersed aqueous phase of ELM in batch system. The experimental data was obtained for 0.5 kmol/m^3 TEA in aqueous dispersed phase of ELM at 300, 500 and 700 rpm of RDC and the mean molar flux of CO_2 for each was calculated by using stoichiometric calculations. **Figure 15** shows the effect of RDC speed on mean molar flux. It was observed that the at 300 rpm the mass transfer rate of CO_2 was $4.96x10^{-4}$ kmol/m^3-s which increased up to $5.48x10^{-4}$ kmol/m^3-s when speed was increased to 700 rpm. Increasing the RDC speed reduces the film thickness over the boundary layer of emulsion droplets, the barriers to the

mass transfer flux are reduced. According to Izatt et al. (1989), film thickness is inversely related to the mechanical energy input or the stirring speed. These results show that increasing the speed of RDC, reduces the thickness of film over the emulsion droplet due to the mechanical energy input. This resulted in increase in rate of mass transfer of CO_2 in the emulsion droplet.

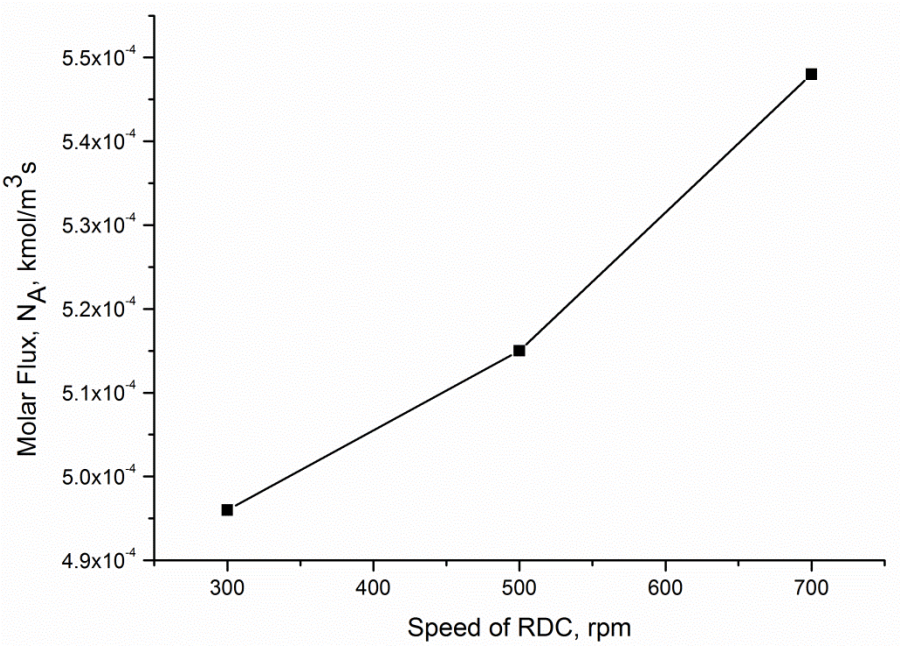

Figure 15. Effect of RDC speed on mean molar flux during the CO_2 absorption in the dispersed aqueous phase of ELM using batch system.

4.2.3. EFFECT OF RUN TIME ON MEAN MOLAR FLUX

According to Kislik (2010) the mass transfer rate or flux of any solute passing through the membrane is a function of distance and time. Littel et al. (1994), reported that the absorption rate of CO_2 in toluene/water emulsion is a function of time. By increasing the time the rate of mass transfer will be increased due to increase in the capacity of absorbent. In this study, the

effect of time over mass transfer rate was determined based on the ELM composition of 1.5 kmol/m^3 TEA at 700 rpm of RDC. **Figure 16** shows that the mass transfer rate linearly decreased with increase in the time for the same concentration of TEA in dispersed aqueous phase of ELM. It is assumed that at short time, the diffusion of feed gas in the dispersed aqueous phase is slow while increasing the time the more gas molecules are diffused in the RDC system.

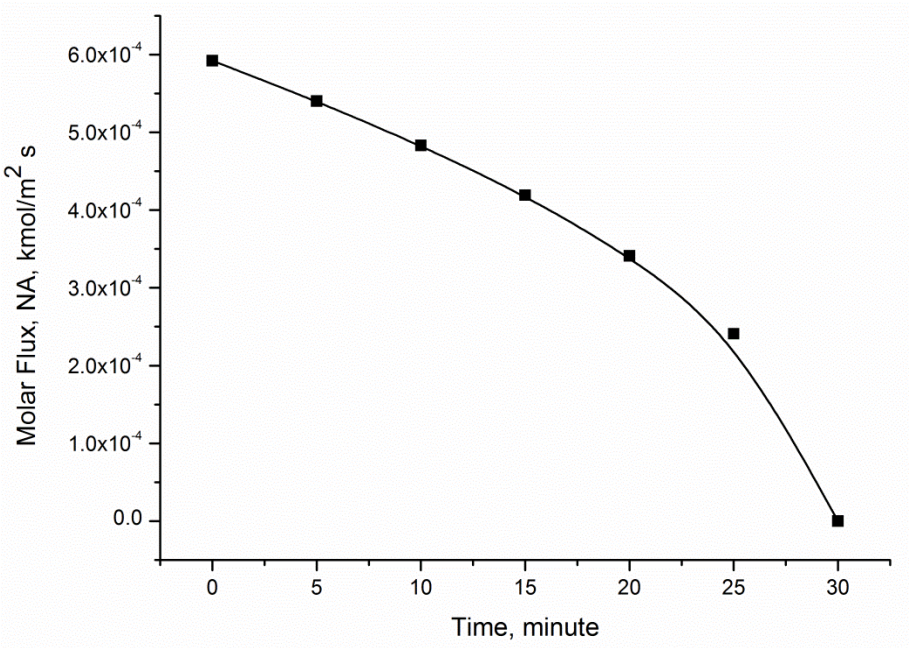

Figure 16. Effect of RDC mean residence time on mean molar flux during the CO_2 absorption in the dispersed aqueous phase of ELM using batch system

4.3. EFFECT OF TEA CONCENTRATION ON MASS TRANSFER COEFFICIENT

The mass transfer coefficient was determined by the absorption rate of CO_2 in dispersed aqueous phase with different concentrations of TEA. Values was determined by using the GC results obtained from RDC system operated at 700 rpm. **Figure 17** shows the effect of 0.5, 1.0

and 1.5 kmol/m^{3}of TEA on mass transfer coefficient of CO_2. It was observed that increasing the concentration of TEA enhanced the mass transfer coefficient of CO_2. It was described that the enhancement factor is functionally related to the concentration of absorbent (Aroonwilas and Tontiwachwuthikul, 1998). It was also reported by Dey and Aroon (Dey and Aroonwilas, 2009) that the higher concentration of MEA causes to increase the value of mass transfer coefficient. Therefore, the results of this study regarding to the effect of TEA concentration over the value of mass transfer coefficient are similar to the previous findings.

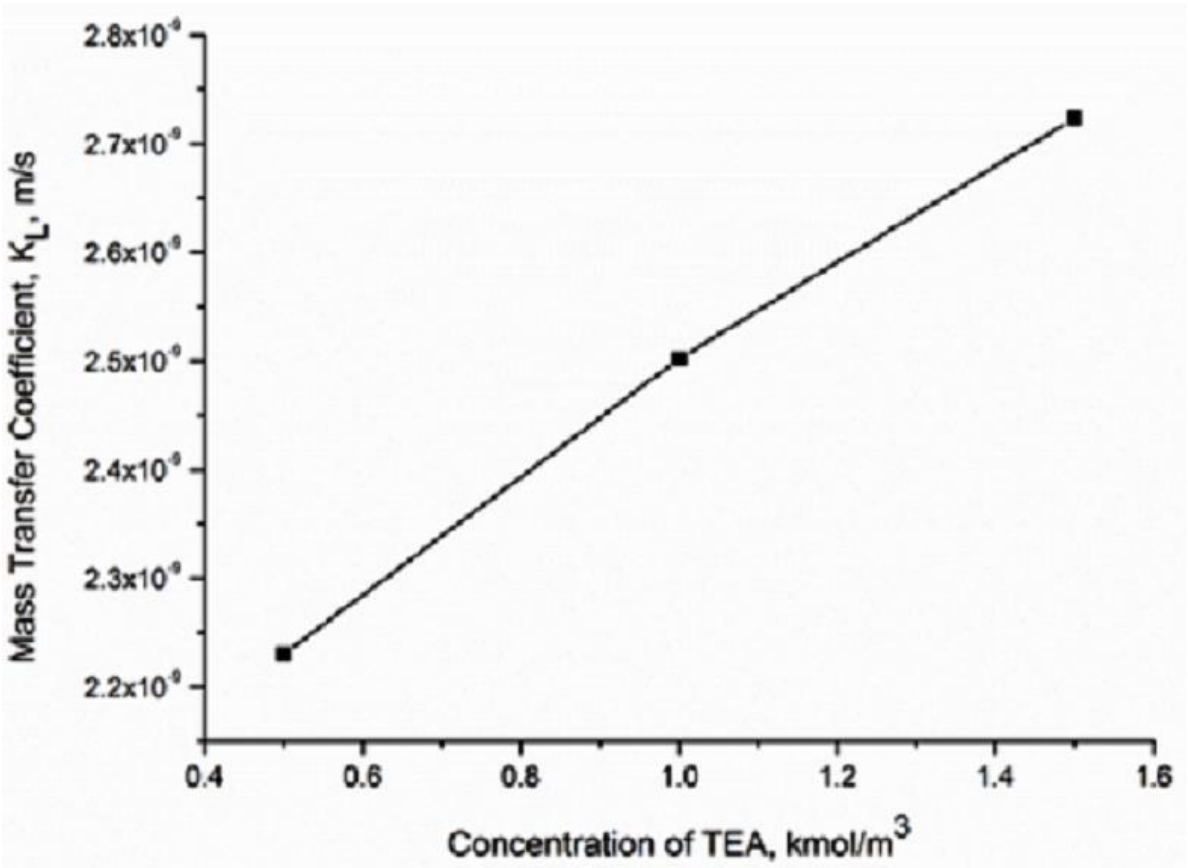

Figure 17. Effect of TEA concentration on mass transfer coefficient.

The increase in mass transfer coefficient by increasing the concentration of TEA in dispersed aqueous phase of ELM is due to the increase in enhancement factor of the system. Enhancement factor increases the efficiency of dispersed aqueous phase of ELM containing TEA to absorb more amount of CO_2.

5. CONCLUSIONS AND RECOMMENDATIONS

The rotating disc contactor (RDC) is an extraction column used in industry because of its simplicity in construction, high throughput, and low power consumption. However, its low performance is its major drawback. This study modified RDC structure to improve its performance for gas liquid system. The hydrodynamic studies indicated that modified design dimensions of RDC applied in this study provided maximum gas liquid contact for ELM and gas system at 700 rpm. According to our studies decreasing the film thickness over the boundary layer of emulsion droplets, the barriers to the mass transfer flux are reduced. Hence the speed of RDC and run time has significant effect on the CO_2 absorption. The results of this study also suggest that the absorption of CO_2 was linearly increased with increase in the speed of RDC from 300 to 700 rpm while the suitable speed of RDC for maximum mass transfer is 500 rpm for 30 minutes. These results show that increasing the speed of RDC, thickness of film over the emulsion droplet decreased due to the mechanical energy input. Therefore, the mass transfer rate of CO_2 in the emulsion droplet increased.

At 500 rpm of RDC, ELM containing 1 kmol/m^3 TEA absorbed 5.6 kmol/m^3 of CO_2. Further increasing the concentration of TEA in the ELM to 1.5 kmol/m^3 resulted in only slight increase in the rate of mass transfer of CO_2. High concentration of TEA makes the ELM more effective

to diffuse CO_2 in the ELM, but it decreases the stability of emulsion due to increase in the interfacial surface tension of the emulsion droplet. Therefore, it is necessary to select the concentration of TEA according to the stability characteristic of ELM. Our study suggested that 1 kmol/m^3 of TEA is highly suitable in ELM according to its stability, since the rate of mass transfer of CO_2 was $5.9x10^{-4}$ kmol/m^2.s. The mass transfer rate was linearly decreased with increasing the time for the same concentration of TEA in dispersed aqueous phase of ELM in RDC. By increasing the time the rate of mass transfer will be increased due to increase in the capacity of absorbent. The increase in mass transfer coefficient by increasing the concentration of TEA in dispersed aqueous phase of ELM is due to the increase in enhancement factor of the system. Enhancement factor increases the efficiency of dispersed aqueous phase of ELM containing TEA to absorb more amount of CO_2. Increasing the amine concentration in dispersed phase of ELM, the amount of CO_2 absorption increased with respect to its volume. It also proved that smaller droplets of ELM provide large surface area to absorb more amount of CO_2 in the RDC system.

Membrane processes are major competitive of conventional amine absorption technology for CO_2 capture from natural gas separation process. If all these parameters are applied in proper conditions of RDC system can be deployed to separate CO_2 from natural gas replacing the traditional amine absorption commonly used to remove CO_2 from natural gas.

REFERENCES

Aksamija, E., Weinländer, C., Sarzio, R., Siebenhofer, M., 2015. The Taylor-Couette Disc Contactor: A Novel Apparatus for Liquid/Liquid Extraction. Separation Science and Technology 50, 2844-2852.

Albal, R.S., Shah, Y.T., Schumpe, A., Carr, N.L., 1983. Mass transfer in multiphase agitated contactors. The Chemical Engineering Journal 27, 61-80.

Aroonwilas, A., Tontiwachwuthikul, P., 1998. Mass Transfer Coefficients and Correlation for CO2 Absorption into 2-Amino-2-methyl-1-propanol (AMP) Using Structured Packing. Industrial & Engineering Chemistry Research 37, 569-575.

Bart, H.J., 2003. Reactive Extraction In Stirred Columns – A Review. Chemical Engineering & Technology 26, 723-731.

Brogren, C., Karlsson, H.T., 1997. Modeling the absorption of SO2 in a spray scrubber using the penetration theory. Chemical Engineering Science 52, 3085-3099.
Chaudhari, R.V., Gholap, R.V., Emig, G., Hofmann, H., 1987. Gas -Liquid mass transfer in 'Dead-End' autoclave reactors. Canadian Journal of Chemical Engineering 65, 744-751.
Chen, H., Sun, Z., Song, X., Yu, J., 2016. A pseudo-3D model with 3D accuracy and 2D cost for the CFD–PBM simulation of a pilot-scale rotating disc contactor. Chemical Engineering Science 139, 27-40.
Dey, A., Aroonwilas, A., 2009. CO2 absorption into MEA-AMP blend: Mass transfer and absorber height index. Energy Procedia 1, 211-215.
Donaldson, T.L., Nguyen, Y.N., 1980. Carbon Dioxide Reaction Kinetics and Transport in Aqueous Amine Membranes. Industrial & Engineering Chemistry Fundamentals 19, 260-266.
Hagewiesche, D.P., Ashour, S.S., Al-Ghawas, H.A., Sandall, O.C., 1995. Absorption of carbon dioxide into aqueous blends of monoethanolamine and N-methyldiethanolamine. Chemical Engineering Science 50, 1071-1079.
Higbie, R., 1935a. Penetration theory leads to use of the contact time in the calculation of the mass transfer coefficients in the two film theory. Trans. Am. Inst. Chem. Engrs 31 365.
Higbie, R., 1935b. The rate of absorption of a pure gas into still liquid during short periods of exposure.
Izatt, R.M., Bruening, R.L., Bruening, M.L., LindH, G.C., Christensen, J.J., 1989. Modeling diffusion-limited, neutral-macrocycle-mediated cation transport in supported liquid membranes. Analytical Chemistry 61, 1140-1148.
Joshi, J.B., Pandit, A.B., Sharma, M.M., 1982. Mechanically agitated gas-liquid reactors. Chemical Engineering Science 37, 813-844.
Karandikar, B.M., Morsi, B.I., Shah, Y.T., Carr, N.L., 1986. Effect of water on the solubility and mass transfer coefficients of CO and H2 in a Fischer-Tropsch liquid. The Chemical Engineering Journal 33, 157-168.
Kislik, V.S., 2010. Bulk Hybrid Liquid Membrane with Organic Water-Immiscible Carriers: Application to Chemical, Biochemical, Pharmaceutical, and Gas Separations, in: Vladimir, S.K. (Ed.), Liquid Membranes. Elsevier, Amsterdam, pp. 201-275.
Ledakowicz, S., Nettelhoff, H., Deckwer, W.D., 1984. Gas-liquid mass transfer data in a stirred autoclave reactor. Industrial and Engineering Chemistry Fundamentals 23, 510-512.
Lekhal, A., Chaudhari, R.V., Wilhelm, A.M., Delmas, H., 1997 Gas-liquid mass transfer in gas-liquid-liquid dispersions Chemical Engineering Science 52, 4069-4077.
Levenspiel, O., Smith, W.K., 1995. Notes on the diffusion-type model for the longitudinal mixing of fluids in flow. Chemical Engineering Science 50, 3891-3896.
Lin, C.-C., Chen, B.-C., 2007. Carbon Dioxide Absorption into NaOH Solution in a Cross-flow Rotating Packed Bed. Journal of Industrial Engineering Chemistry 13, 1083-1090.
Lin, C.-C., Chen, B.-C., Chen, Y.-S., Hsu, S.-K., 2008. Feasibility of a cross-flow rotating packed bed in removing carbon dioxide from gaseous streams. Separation and Purification Technology 62, 507-512.
Littel, R.J., Versteeg, G.F., Swaaij van, W.P.M., 1994. Physical absorption of CO2 and propene into toluene/water emulsions. AIChE Journal 40, 1629-1638.
Logsdail, D.H., Thornton, J.D., Pratt, H.R.C., 1957. Liquid-liquid extraction Part XII Flooding rates and performance data for a rotary disc contactor. Trans. Inst. Chem. Engrs. 35, 301-315.
Miyauchi, T., Vermeulen, T., 1963. Longitudinal Dispersion in Two-Phase Continuous-Flow Operations. Industrial & Engineering Chemistry Fundamentals 2, 113-126.
Mohanty, S., 2000. MODELING OF LIQUID-LIQUID EXTRACTION COLUMN: A REVIEW, Reviews in Chemical Engineering, p. 199.
Morís, M.A., Díez, F.V., Coca, J., 1997. Hydrodynamics of a rotating disc contactor. Separation and Purification Technology 11, 79-92.
Park, S.W., Choi, B.S., Kim, T.Y., Lee, J.W., 2004. Chemical absorption of carbon dioxide with NaOH in non-Newtonian w/o emulsion, in: Sang, E.P., Chang, J.S., Kyu Wan, L. (Eds.), Studies in Surface Science and Catalysis. Elsevier, pp. 523-526.
Park, S.W., Choi, B.S., Lee, J.W., 2006. Chemical absorption of carbon dioxide with triethanolamine in non-aqueous solutions. Korean Journal of Chemical Engineering 23, 138-143.
Park, S.W., Choi, B.S., Lee, J.W., 2008. Chemical absorption of carbon dioxide into aqueous elastic xanthan gum solution containing NaOH. Journal of Industrial and Engineering Chemistry 14, 303-307.
Poncin, S., Nguyen, C., Midoux, N., Breysse, J., 2002. Hydrodynamics and volumetric gas-liquid mass transfer coefficient of a stirred vessel equipped with a gas-inducing impeller. Chemical Engineering Science 57, 3299-3306.
Rubia, M.D.L., García-Abuín, A., Gómez-Díaz, D., Navaza, J.M., 2010. Interfacial area and mass transfer in carbon dioxide absorption in TEA aqueous solutions in a bubble column reactor. Chemical Engineering and Processing: Process Intensification 49, 852-858.
Sleicher, C.A., 1959. Axial mixing and extraction efficiency. AIChE Journal 5, 145-149.
Stevens, G.W., Lo, T.C., Baird, M.H.I., 2000. Extraction, Liquid-Liquid, Kirk-Othmer Encyclopedia of Chemical Technology. John Wiley & Sons, Inc.
Strand, C.P., Olney, R.B., Ackerman, G.H., 1962. Fundamental aspects of rotating disk contactor performance. AIChE Journal 8, 252-261.
Takahshi, K., Nii, S., Kawaizumi, F., 2005. Absorption Rate of Carbon Dioxide by K2CO3-KHCO3 DEA Aqueous Solution. Developments in Chemical Engineering and Mineral Processing 13, 159-176.
Tedajo, G.M., Seiller, M., Prognon, P., Grossiord, J.L., 2001. pH compartmented w/o/w multiple emulsion: a diffusion study. Journal of Controlled Release 75, 45-53.
Vikhansky, A., Kraft, M., 2004. Modelling of a RDC using a combined CFD-population balance approach. Chemical Engineering Science 59, 2597-2606.
Vladimir, S.K., 2010. Carrier-Facilitated Coupled Transport Through Liquid Membranes: General Theoretical Considerations and Influencing Parameters, in: Vladimir, S.K. (Ed.), Liquid Membranes. Elsevier, Amsterdam, pp. 17-71.
Wan, Y., Wang, X., Zhu, B., Zhang, X., 2001. Development of a new series of polyamine-type polymeric surfactants used for emulsion liquid membranes. Journal of Membrane Science 184, 49-57.
Zhang, S.H., Yu, S.C., Zhou, Y.C., Su, Y.F., 1985. A model for liquid-liquid extraction column performance — The influence of drop size distribution on extraction efficiency. The Canadian Journal of Chemical Engineering 63, 212-226.